

# A Generalized Unit System for Concise Electromagnetic Formulation and Accurate Numerical Solutions

L. Vu-Quoc,<sup>1</sup> V. Srinivas,<sup>2</sup> and Y. Zhai<sup>3</sup>

*Aerospace Engineering, Mechanics & Engineering Science, University of Florida, Gainesville, Florida 32611*

E-mail: vu-quoc@ufl.edu

Received August 23, 2001; revised April 23, 2002

---

We present in this paper a novel generalized unit system (GUS) for electromagnetic formulation and for improving the numerical behavior of the solution procedure by decreasing the condition number of the finite element (FE) matrices. The goal is to express, in the GUS, the governing electromagnetic equations in a form that does not involve any factors such as  $4\pi$  and those related to the physical properties of vacuum. This goal is achieved by scaling all physical quantities. The scaling factors are not all free parameters, but are constrained by specific relations. We prove that there are only two free parameters, but only one is significant for minimizing the condition number of the FE matrices. Numerical examples are presented to illustrate the essential features of the proposed GUS, including the minimization of the condition number. © 2002 Elsevier Science (USA)

---

## 1. INTRODUCTION

With the ever-increasing operating frequencies in power electronics, there is a growing demand to accurately solve coupled electromagnetic problems [1]. An accurate computer model of electromagnetic devices is crucial to reduce their cost and to improve their design. Electric and magnetic fields in an electromagnetic device are solutions to Maxwell's equations, which can be expressed in many unit systems. The choice of the unit system depends on the type of application [2, 3]. On the other hand, the commonly used unit systems often lead to ill-conditioned finite element (FE) matrices due to large changes in the material properties

<sup>1</sup> Professor. URL: [www.aero.ufl.edu/~vql](http://www.aero.ufl.edu/~vql).

<sup>2</sup> Former Graduate Research Assistant; now with Sequence Design, Inc. after a stint at the Stanford Linear Accelerator Center.

<sup>3</sup> Graduate Research Assistant.

[4, 5], in particular the conductivity, as well as the characteristics of the element geometric dimensions of the FE model, such as poor aspect ratio. For power electronic devices functioning at the frequency of interest, in the SI unit system, the numerical values of the terms related to the electric current dominate those that are related to the other physical processes. As the electric current is only present inside the conductor (e.g., the winding wire for a power transformer), the terms of the FE matrix inside the conductor are much larger than those outside the conductor, thereby leading to a large condition number in the resulting FE matrix. This numerical ill-conditioning often makes the analysis impossible (see, e.g., [4] and the examples in this work). In the past, some researchers have suggested the use of scaling. In [6], the use of a volt, ohm, meter, and second (VOMS) unit system was suggested. Unlike our proposed generalized unit system (GUS), the VOMS unit system cannot, however, be modified to account for a change in the excitation frequency and in the material properties.

To decrease the condition number of the FE matrices resulting from the discretization of the time-harmonic coupled electromagnetic (EM) problems, and hence to improve the numerical behavior of the FE solution procedure, we propose in this paper a multiple-scale technique, to transform Maxwell's equations to a generalized unit system, where the EM quantities are nondimensionalized. The technique requires a set of scaling parameters that are determined by the physics of the electromagnetic problem. The constant coefficients (e.g.,  $4\pi$ , etc.) in Maxwell's equations and in the constitutive laws are eliminated since they are absorbed into the field quantities in the scaling process. The physical meaning and the numerical values of the electric and magnetic field quantities in the GUS depend on two primary scaling parameters. A suitable choice of these two primary scaling parameters shifts the focus of the problem away from the dominating effect of the conductors and, as a consequence, reduces the condition number in the FE matrices, thus significantly improving the accuracy. Moreover, the scaled Maxwell equations are more convenient for problem formulation and for subsequent mathematical analysis. Scaling proves to be particularly useful for modeling electromagnetic devices having a complex geometry and a mixture of regions of finite conductivity and zero conductivity. We demonstrate the efficacy of this scaling technique in a FE model for a single cell of an advanced multilayer ceramic capacitor (MLCC) designed by Ngo [7–8]. For example, the condition number of the solution for a single cell in a capacitor (Fig. 1a) with an applied voltage at the left end of the top electrode and at the right end of the bottom electrode can be improved from  $\mathcal{O}(10^{20})$  in the SI unit system to  $\mathcal{O}(10^{13})$

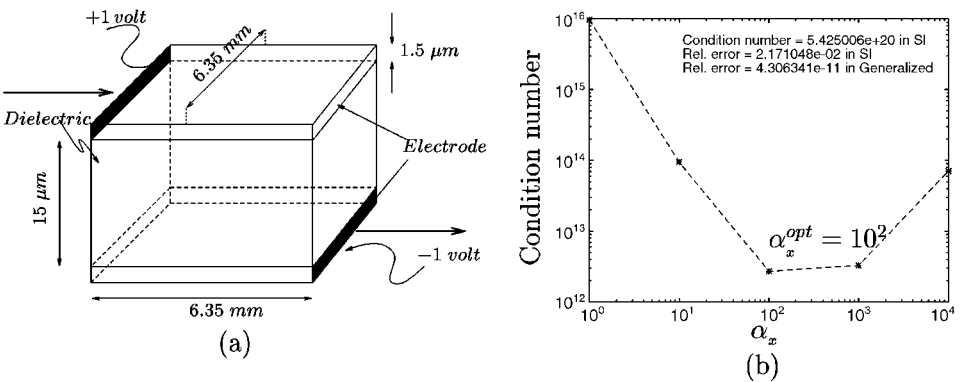


**FIG. 1.** (a) A schematic of one cell in an MLCC (not drawn to scale). The direction of the current flow is indicated by arrows. (b) Condition number vs scaling parameter  $\alpha_x$ .

in the optimal *generalized* unit system (GUS). The relative error<sup>4</sup> improves from  $\mathcal{O}(10^{-2})\%$  to  $\mathcal{O}(10^{-11})\%$ . The choice of the scaling parameter depends on the electromagnetic properties of the materials and the frequency of excitation. The condition number and the relative errors also depend on the boundary conditions. The application of the concept of the GUS to a substantial physics problem was reported in another paper in the analysis of a complex and novel class of advanced multilayer capacitors, in which the use of the GUS is critical [9].

We first review the governing equations for electromagnetic problems in various commonly used unit systems and the FE discrete matrix forms of Maxwell's equations for static, transient, and time-harmonic problems. We then introduce a unit scaling methodology that led to a new *generalized* unit system for improving the matrix condition number of the finite element matrices. Constrained relations and only one primary scaling parameter are proposed for unit conversion. We derive in detail the unit conversion for symbols, for numerical numbers, and for FE matrices. The discussions for static, transient, and time-harmonic problems show how the new unit system can significantly improve the numerical behavior of the solution procedure for EM problems. It should be noted, however, that the application of the proposed GUS is not restricted to the stiff problem encountered in MLCC. For example, Maxwell's equations expressed in the GUS take on a simple form, in which none of the coefficients such as  $4\pi$  and those related to the physical properties of vacuum appear.

A numerical example involving a parallel plate capacitor with poor aspect ratio shows a significant improvement of FE matrix condition number and thus of the accuracy of the results.

## 2. ELECTROMAGNETIC GOVERNING EQUATIONS

### 2.1. EM Equations in RCGS Unit System

The governing equations for a general EM problem in the rationalized CGS (RCGS) units are as follows. First, there are the four Maxwell equations,

$$\text{Faraday's law: } \frac{1}{c} \frac{\partial \mathbf{B}}{\partial t} + \text{curl } \mathbf{E} = \mathbf{0}, \quad (2.1)$$

$$\text{Gauss's law for electric field: } \text{div } \mathbf{D} - \rho_f = 0, \quad (2.2)$$

$$\text{Ampère's law: } -\frac{1}{c} \frac{\partial \mathbf{D}}{\partial t} + \text{curl } \mathbf{H} - \frac{1}{c} \mathbf{J}_f = \frac{1}{c} \mathbf{J}_a, \quad (2.3)$$

$$\text{Gauss's law for magnetic induction: } \text{div } \mathbf{B} = 0, \quad (2.4)$$

where the field quantities are the electric field  $\mathbf{E}$ , the magnetic induction  $\mathbf{B}$ , the electric induction  $\mathbf{D}$ , and the magnetic field  $\mathbf{H}$ . The quantities  $\mathbf{J}_f$  and  $\rho_f$  are the field induced free-current volume density and free-charge volume density, respectively. In some electromagnetic problems an applied free-current volume density  $\mathbf{J}_a$  is prescribed. In addition there are the two constitutive laws,

$$\mathbf{D} = \mathbf{E} + \mathbf{P}, \quad \mathbf{H} = \mathbf{B} - \mathbf{M}, \quad (2.5)$$

<sup>4</sup> Here, the numerical accuracy of the solution of a linear system of equations  $\mathbf{K}d = f$  is estimated by the relative error

$$\frac{\|\mathbf{K}d - f\|_2}{\|f\|_2},$$

where  $\mathbf{K}$  is a square matrix and  $f$  is the right-hand-side column vector. The computed solution is represented by the column vector  $d$ .

and the force-field relationship and Newton’s second law,

$$\mathbf{f} = \rho_f \mathbf{E} + \frac{1}{c} \mathbf{J}_f \times \mathbf{B}, \quad \mathbf{F} = m \ddot{\mathbf{x}}, \tag{2.6}$$

where  $\mathbf{f}$ ,  $\mathbf{F}$ ,  $m$ , and  $\ddot{\mathbf{x}}$  represent the force vector per unit volume, force vector, mass, and acceleration vector, respectively.

### 2.2. EM Equations in Various Unit Systems

We summarize the aforementioned EM governing equations in various unit system historically developed for EM field problems [2, 3] in Table I, which lists the four CGS (centimeter, gram, and second) systems—the electrostatic system (CGS esu), the electromagnetic system (CGS emu), the Gaussian system, unrationalized (CGS Gaussian), and the Heaviside–Lorentz rationalized system (CGS Heaviside–Lorentz); the most commonly

**TABLE I**  
Maxwell Equations in Different Unit Systems

| Unit system                             | $\mathbf{D}, \mathbf{H}$  | Maxwell equations  |   |
|---|---|--|---|
| CGS esu                                 | $\mathbf{D} = \mathbf{E} + 4\pi \mathbf{P}$<br>$\mathbf{H} = c^2 \mathbf{B} - 4\pi \mathbf{M}$              | $\text{div } \mathbf{D} = 4\pi \rho_f,$<br>$\text{div } \mathbf{B} = 0,$ | $\text{curl } \mathbf{H} = 4\pi \mathbf{J}_f + \frac{\partial \mathbf{D}}{\partial t}$<br>$\text{curl } \mathbf{E} + \frac{\partial \mathbf{B}}{\partial t} = 0$<br>$\mathbf{f} = \rho_f \mathbf{E} + \mathbf{J}_f \times \mathbf{B}$   |
| CGS emu                                 | $\mathbf{D} = \frac{1}{c^2} \mathbf{E} + 4\pi \mathbf{P}$<br>$\mathbf{H} = \mathbf{B} - 4\pi \mathbf{M}$    | $\text{div } \mathbf{D} = 4\pi \rho_f,$<br>$\text{div } \mathbf{B} = 0,$ | $\text{curl } \mathbf{H} = 4\pi \mathbf{J}_f + \frac{\partial \mathbf{D}}{\partial t}$<br>$\text{curl } \mathbf{E} + \frac{\partial \mathbf{B}}{\partial t} = 0$<br>$\mathbf{f} = \rho_f \mathbf{E} + \mathbf{J}_f \times \mathbf{B}$   |
| CGS Gaussian<br>(unrationalized)        | $\mathbf{D} = \mathbf{E} + 4\pi \mathbf{P}$<br>$\mathbf{H} = \mathbf{B} - 4\pi \mathbf{M}$                  | $\text{div } \mathbf{D} = 4\pi \rho_f,$<br>$\text{div } \mathbf{B} = 0,$ | $\text{curl } \mathbf{H} = \frac{4\pi}{c} \mathbf{J}_f + \frac{1}{c} \frac{\partial \mathbf{D}}{\partial t}$<br>$\text{curl } \mathbf{E} + \frac{1}{c} \frac{\partial \mathbf{B}}{\partial t} = 0$<br>$\mathbf{f} = \rho_f \mathbf{E} + \frac{1}{c} \mathbf{J}_f \times \mathbf{B}$ |
| CGS Heaviside–Lorentz<br>(rationalized) | $\mathbf{D} = \mathbf{E} + \mathbf{P}$<br>$\mathbf{H} = \mathbf{B} - \mathbf{M}$                            | $\text{div } \mathbf{D} = \rho_f,$<br>$\text{div } \mathbf{B} = 0,$      | $\text{curl } \mathbf{H} = \frac{1}{c} \mathbf{J}_f + \frac{1}{c} \frac{\partial \mathbf{D}}{\partial t}$<br>$\text{curl } \mathbf{E} + \frac{1}{c} \frac{\partial \mathbf{B}}{\partial t} = 0$<br>$\mathbf{f} = \rho_f \mathbf{E} + \frac{1}{c} \mathbf{J}_f \times \mathbf{B}$    |
| SI system                               | $\mathbf{D} = \epsilon_0 \mathbf{E} + \mathbf{P}$<br>$\mathbf{H} = \frac{1}{\mu_0} \mathbf{B} - \mathbf{M}$ | $\text{div } \mathbf{D} = \rho_f,$<br>$\text{div } \mathbf{B} = 0,$      | $\text{curl } \mathbf{H} = \mathbf{J}_f + \frac{\partial \mathbf{D}}{\partial t}$<br>$\text{curl } \mathbf{E} + \frac{\partial \mathbf{B}}{\partial t} = 0$<br>$\mathbf{f} = \rho_f \mathbf{E} + \mathbf{J}_f \times \mathbf{B}$  |
| Generalized unit system<br>(GUS)        | $\mathbf{D} = \mathbf{E} + \mathbf{P}$<br>$\mathbf{H} = \mathbf{B} - \mathbf{M}$                            | $\text{div } \mathbf{D} = \rho_f,$<br>$\text{div } \mathbf{B} = 0,$      | $\text{curl } \mathbf{H} = \mathbf{J}_f + \frac{\partial \mathbf{D}}{\partial t}$<br>$\text{curl } \mathbf{E} + \frac{\partial \mathbf{B}}{\partial t} = 0$<br>$\mathbf{f} = \rho_f \mathbf{E} + \mathbf{J}_f \times \mathbf{B}$  |

*Note.* The universal constants are the speed of light in vacuum  $c = 2.99792458 \times 10^{10}$  cm/s, the permittivity of free space  $\epsilon_0 = 1/(36\pi) \times 10^{-9}$  SI units, and the permeability of free space  $\mu_0 = 4\pi \times 10^{-7}$  SI units.

used SI unit system, which is the same as the rationalized MKSA (meter, kilogram, second, and ampere) system; and the governing equations in the *generalized* unit system, which are similar, except that the factor  $1/c$  is omitted.

### 3. GALERKIN FE PROJECTION (SI UNIT SYSTEM)

The use of FE analysis to model electromagnetic components is well established, e.g., [10, 11]. The principle of virtual power for electromagnetics [12] is the basis for the approximation. A detailed discussion of the FE procedure can be found in [13] and [14]. Here we present the discrete matrix form of Maxwell's equations after a Galerkin FE projection in terms of potentials in the SI unit system. The present formulation uses the magnetic vector potential  $\mathbf{A}$  together with the time-integrated scalar potential  $\psi$  [15].

#### 3.1. Maxwell Equations in Terms of Potentials

The following definition of the potentials  $\mathbf{A}$  and  $\psi$  [15]

$$\mathbf{B} =: \text{curl } \mathbf{A}, \quad \mathbf{E} =: -\text{grad} \frac{\partial \psi}{\partial t} - \frac{\partial \mathbf{A}}{\partial t}, \quad (3.1)$$

satisfy Faraday's law and Gauss's law for magnetic induction. Therefore, the partial differential equations to be solved for the electromagnetic problem formulated using potentials  $\mathbf{A}$  and  $\psi$  are

$$\text{curl } \mathbf{H} - \frac{\partial \mathbf{D}}{\partial t} - \mathbf{J}_f = \mathbf{J}_a, \quad \text{div } \mathbf{D} - \rho_f = 0, \quad (3.2)$$

where all the expressions on the left-hand side must be represented in terms of these potentials and where  $\mathbf{J}_a$  is the applied source.

The part of the volume  $\Omega$  in which the current density  $\mathbf{J}_f$  is not zero in the presence of a nonzero electric field  $\mathbf{E}$  is characterized as a region of finite conductivity, and is designated to be  $\Omega_{\text{cond}} \subset \Omega$ . Because the focus of the present work does not apply to superconductors, we designate the remaining volume ( $\Omega \setminus \Omega_{\text{cond}}$ ) to be the nonconductive region.

The field quantities  $\mathbf{H}$ ,  $\mathbf{D}$ , and  $\mathbf{J}_f$  are related to the potentials defined in (3.1) via the constitutive equations

$$\mathbf{D} = \epsilon_0 \mathbf{E} + \mathbf{P}(\mathbf{E}), \quad \mathbf{H} = \frac{1}{\mu_0} \mathbf{B} - \mathbf{M}(\mathbf{B}), \quad \mathbf{J}_f \equiv \mathbf{J}_f(\mathbf{E}), \quad (3.3)$$

where the polarization  $\mathbf{P}$  is a nonlinear function of the electric field  $\mathbf{E}$ , and the magnetization  $\mathbf{M}$  is a nonlinear function of the magnetic induction  $\mathbf{B}$ . Here, we assume linear-isotropic constitutive relationships, i.e., the relations in (3.3) take the form

$$\mathbf{D} = \epsilon(\mathbf{x}) \mathbf{E}, \quad \mathbf{H} = \frac{1}{\mu(\mathbf{x})} \mathbf{B}, \quad \mathbf{J}_f = \sigma(\mathbf{x}) \mathbf{E}, \quad (3.4)$$

where the permittivity  $\epsilon$ , permeability  $\mu$ , and conductivity  $\sigma$  are functions only of position  $\mathbf{x}$ .

### 3.2. FE Discrete Maxwell Equations

#### 3.2.1. Static Problems

The FE matrix equation for an electrostatic problem derived from Gauss's law for electric fields (2.2) is

$$[M^{\psi\psi}]\{\dot{\psi}_0\} = \{F^{\psi_0}\}, \quad (3.5)$$

where  $M_{IJ}^{\psi\psi} = \int_{\Omega \setminus \Omega_{\text{cond}}} \epsilon (\text{grad } N_I) \cdot (\text{grad } N_J) d\Omega$ . Note that  $N_I$  and  $N_J$  are finite element interpolation functions associated with nodes  $I$  and  $J$ , respectively.

The FE matrix equation for the magnetostatic problem derived from Ampère's law (2.3) at static condition is

$$[K^{AA}]\{\mathcal{A}_0\} = \{F^{A_0}\}. \quad (3.6)$$

The "stiffness" matrix  $K^{AA}$  can be partitioned into submatrices  $K_{IJ}^{AA} \in \mathbb{R}^{3 \times 3}$ , with

$$K_{IJ}^{AA} := \int_{\Omega} \frac{1}{\mu} (\text{grad } N_I \cdot \text{grad } N_J) \mathbb{I} d\Omega - \int_{\Omega} \frac{1}{\mu} (\text{grad } N_J \otimes \text{grad } N_I) d\Omega \in \mathbb{R}^{3 \times 3}, \quad (3.7)$$

where  $\mathbb{I} \in \mathbb{R}^{3 \times 3}$  is the identity matrix.

In summary, the matrix equation for the static case is stated as

$$\text{Find } \mathcal{A}_0 \in \mathbb{R}^{(3n_{A_0} \times 1)} \text{ and } \dot{\psi}_0 \in \mathbb{R}^{(n_{\psi_0} \times 1)} \text{ such that} \quad (3.8)$$

$$\begin{bmatrix} K^{AA} & 0 \\ 0 & M^{\psi\psi} \end{bmatrix} \begin{Bmatrix} \mathcal{A}_0 \\ \dot{\psi}_0 \end{Bmatrix} = \begin{Bmatrix} F^{A_0} \\ F^{\psi_0} \end{Bmatrix},$$

where  $\mathcal{A}_0$  contains the unknown degrees of freedom corresponding to the vector potential  $\mathbf{A}_0$ , and  $\dot{\psi}_0$  contains the unknown degrees of freedom corresponding to the scalar potential  $\dot{\psi}_0$ . The matrix  $K^{AA} \in \mathbb{R}^{(3n_{A_0} \times 3n_{A_0})}$  and  $M^{\psi\psi} \in \mathbb{R}^{(n_{\psi_0} \times n_{\psi_0})}$  are symmetric and positive semidefinite.<sup>5</sup> The number  $n_{A_0}$  corresponds to the number of nodes at which the vector potential  $\mathbf{A}_0$  is to be determined, and the number  $n_{\psi_0}$  corresponds to the number of nodes at which the scalar potential  $\dot{\psi}_0$  is to be determined.

#### 3.2.2. Transient Problems

The FE matrix equation for the transient problem is derived from Ampère's law (3.2)<sub>1</sub> and the time-integrated continuity equation

$$\frac{\partial(\text{div } \mathbf{D})}{\partial t} + \text{div}[\mathbf{J}_f + \mathbf{J}_a] = 0. \quad (3.9)$$

<sup>5</sup> For piecewise constant material properties, two-point Gauss integration is used to calculate the entries in the matrices  $K^{AA}$  and  $M^{\psi\psi}$ . Numerical experiments show that no significant improvement in accuracy is achieved with more Gauss points.

Equations (3.2)<sub>1</sub> and (3.9) can be expressed in the form

$$\underbrace{\begin{Bmatrix} -\frac{\partial \mathbf{D}}{\partial t} \\ \frac{\partial}{\partial t}(\operatorname{div} \mathbf{D}) \end{Bmatrix}}_{\substack{\text{second order} \\ \text{in time}}} + \underbrace{\begin{Bmatrix} -\mathbf{J}_f \\ (\operatorname{div} \mathbf{J}_f) \end{Bmatrix}}_{\substack{\text{first order} \\ \text{in time}}} + \underbrace{\begin{Bmatrix} \operatorname{curl} \mathbf{H} \\ 0 \end{Bmatrix}}_{\substack{\text{zeroth order} \\ \text{in time}}} = \underbrace{\begin{Bmatrix} \mathbf{J}_a \\ -\operatorname{div} \mathbf{J}_a \end{Bmatrix}}_{\text{force}}, \quad (3.10)$$

where the quantities are grouped according to the order of the derivatives of the potentials  $\mathbf{A}$  and  $\psi$  with respect to time. To express the fields in terms of the vector potential  $\mathbf{A}$  and the time-integrated scalar potential  $\psi$ , recall that  $\mathbf{H} = \frac{1}{\mu} \mathbf{B} = \frac{1}{\mu} \operatorname{curl} \mathbf{A}$ , and

$$\mathbf{D} = \epsilon \mathbf{E} = \epsilon \left( -\operatorname{grad} \frac{\partial \psi}{\partial t} - \frac{\partial \mathbf{A}}{\partial t} \right), \quad \mathbf{J}_f = \sigma \mathbf{E} = \sigma \left( -\operatorname{grad} \frac{\partial \psi}{\partial t} - \frac{\partial \mathbf{A}}{\partial t} \right).$$

Equation (3.10) can be expressed in matrix form after a FE discretization as

$$M\ddot{d} + B\dot{d} + Kd = F, \quad (3.11)$$

where  $d := \{\psi^A\}$  and the matrices  $M$ ,  $B$ , and  $K$  are referred to as ‘‘mass,’’ ‘‘damping,’’ and ‘‘stiffness’’ matrices, respectively. The semidiscrete system (3.11) can be solved using the Newmark method, in which the ‘‘dynamic stiffness’’ matrix

$$[\mathbb{K}] := \left( \frac{1}{(\Delta t_{n+1})^2} M + \frac{\gamma}{\Delta t_{n+1}} B + K \right) \quad (3.12)$$

is inverted at each time step. The quantities  $\beta$  and  $\gamma$  are two parameters in the Newmark algorithm, and  $\Delta t_{n+1} = t_{n+1} - t_n$  is the time step size.

The matrices can be conveniently partitioned as a mass matrix, a damping matrix, and a stiffness matrix,

$$M = \begin{bmatrix} M^{AA} & M^{A\psi} \\ M^{\psi A} & M^{\psi\psi} \end{bmatrix}, \quad B = \begin{bmatrix} B^{AA} & B^{A\psi} \\ B^{\psi A} & B^{\psi\psi} \end{bmatrix}, \quad K = \begin{bmatrix} K^{AA} & 0 \\ 0 & 0 \end{bmatrix}, \quad (3.13)$$

where the superscripts  $A$  and  $\psi$  correspond to the potentials  $\mathbf{A}$  and  $\psi$ , respectively. Hence, from (3.12), the dynamic stiffness matrix on the left-hand side in the Newmark method is

$$\left( \frac{1}{(\Delta t_{n+1})^2} \begin{bmatrix} M^{AA} & M^{A\psi} \\ M^{\psi A} & M^{\psi\psi} \end{bmatrix} + \frac{\gamma}{\Delta t_{n+1}} \begin{bmatrix} B^{AA} & B^{A\psi} \\ B^{\psi A} & B^{\psi\psi} \end{bmatrix} + \begin{bmatrix} K^{AA} & 0 \\ 0 & 0 \end{bmatrix} \right). \quad (3.14)$$

Each of these matrices can be partitioned into  $N \times N$  submatrices, where  $N$  represents the number of basis functions used. For example, the expression in the weak form related to the term  $\frac{\partial \mathbf{D}}{\partial t}$  in (3.10) is

$$\begin{aligned} & \int_{\Omega} \epsilon \left( -\operatorname{grad} \frac{\partial \psi}{\partial t} - \frac{\partial \mathbf{A}}{\partial t} \right) \cdot \mathbf{W}_A \, d\Omega \\ & \quad \text{related to } M^{A\psi} \\ & = \overbrace{\int_{\Omega} \epsilon \left( -\operatorname{grad} \frac{\partial \psi}{\partial t} \right) \cdot \mathbf{W}_A \, d\Omega}^{\text{related to } M^{A\psi}} + \underbrace{\int_{\Omega} \epsilon \left( -\frac{\partial \mathbf{A}}{\partial t} \right) \cdot \mathbf{W}_A \, d\Omega}_{\text{related to } M^{AA}}. \end{aligned} \quad (3.15)$$

The second term on the right-hand side of (3.15) can be partitioned into submatrices of the form

$$M_{IJ}^{AA} := \left( \int_{\Omega} \epsilon(N_I N_J) d\Omega \right) \mathbb{I} \in \mathbb{R}^{3 \times 3}, \quad (3.16)$$

where  $\mathbb{I} \in \mathbb{R}^{3 \times 3}$  is the identity matrix. The remaining matrices in  $M$  and  $B$  in (3.13) and the corresponding  $N \times N$  submatrices can be expressed as

$$\begin{aligned} [{}_{\kappa}]Y_{IJ}^{AA} &:= \left( \int_{\Omega} \kappa(N_I N_J) d\Omega \right) \mathbb{I} \in \mathbb{R}^{3 \times 3}, & [{}_{\kappa}]Y_{IJ}^{\psi\psi} &:= \int_{\Omega} \kappa(\text{grad } N_I \cdot \text{grad } N_J) d\Omega \in \mathbb{R}^{1 \times 1}, \\ [{}_{\kappa}]Y_{IJ}^{A\psi} &:= \int_{\Omega} \kappa(N_I (\text{grad } N_J)) d\Omega \in \mathbb{R}^{3 \times 1}, & [{}_{\kappa}]Y_{IJ}^{\psi A} &:= \int_{\Omega} \kappa((\text{grad } N_I) N_J) d\Omega \in \mathbb{R}^{1 \times 3}, \end{aligned} \quad (3.17)$$

where  $[{}_{\kappa}]Y$  represents the  $M$  or  $B$  matrix and  $\kappa$  represents the permittivity  $\epsilon$  or conductivity  $\sigma$  for the  $M$  or  $B$  matrix, respectively. The “stiffness” matrix partitioned into submatrices  $K_{IJ}^{AA} \in \mathbb{R}^{3 \times 3}$  has the same expression as in the static case in (3.7).

### 3.2.3. Time-Harmonic Problems

A convenient formulation for time-harmonic problems is to represent all quantities as time-harmonic functions of the frequency  $\omega$ ; i.e., the potentials are  $\mathbf{A}(\mathbf{x}, t) := \bar{\mathbf{A}}_0(\mathbf{x})e^{i\omega t}$  and  $\psi(\mathbf{x}, t) := \bar{\psi}_0(\mathbf{x})e^{i\omega t}$ . Hence, we only need to calculate the complex functions  $\bar{\mathbf{A}}_0$  and  $\bar{\psi}_0$  that are independent of time  $t$ . We determine the electric and magnetic field quantities for a prescribed distribution of current (specified by  $\bar{\mathbf{J}}_a$ ) and a prescribed voltage (specified by  $-i\omega\bar{\psi}_{a_0}$ ), with appropriate boundary conditions.

The set of linear equations to be solved for the time-harmonic problem involves the stiffness matrix

$$\mathbb{K} = \begin{bmatrix} {}^r K - (\omega^2) {}^r M & (\omega) {}^i B \\ -(\omega) {}^r B & {}^i K - (\omega^2) {}^i M \end{bmatrix}, \quad (3.18)$$

where  $\omega$  is the frequency of the driving voltage. The condition number of this time-harmonic stiffness matrix determines the accuracy of the solution. The “mass” matrices ( ${}^r M$ ,  ${}^i M$ ) are positive definite. The “damping” matrices ( ${}^r B$ ,  ${}^i B$ ) and the “stiffness” matrices ( ${}^r K$ ,  ${}^i K$ ) are positive semidefinite. These matrices (partitioned into submatrices) can be expressed as

$$\theta Y := \begin{bmatrix} \theta Y^{AA} & \theta Y^{A\psi} \\ \theta Y^{\psi A} & \theta Y^{\psi\psi} \end{bmatrix} \in \mathbb{R}^{((3n_{A_0} + n_{\psi_0}) \times (3n_{A_0} + n_{\psi_0}))}, \quad (3.19)$$

where  $Y$  represents the  $M$ ,  $B$ , or  $K$  matrix and the prefix  $\theta$  represents “r” or “i”, which indicates whether the matrix is associated with the real part or with the imaginary part of the potentials, respectively. The numbers  $n_{A_0}$  ( $n_{A_r}$  and  $n_{A_i}$ ) correspond to the numbers of nodes at which the real and imaginary parts of the vector potential  $\bar{\mathbf{A}}$  are to be determined. The numbers  $n_{\psi_0}$  ( $n_{\psi_r}$  and  $n_{\psi_i}$ ) correspond to the numbers of nodes at which the real and imaginary parts of the scalar potential  $\bar{\psi}$  are to be determined.



#### 4. UNIT SCALING METHODOLOGY

To achieve the goal of an optimal condition number in the resulting FE matrices, we introduce a novel generalized unit system to obtain simple Maxwell's equations without a  $4\pi$  factor and factors related to physical properties of vacuum. We first introduce 12 multiplicative factors to transform the 12 EM quantities involved in the EM governing equations from the rationalized CGS unit system to the *generalized* unit system (abbreviated both as GUS and GEN); we then show that these 12 scaling factors are not free but are constrained by 11 nonlinear constrained relations, which lead to only two independent scaling factors. By fixing the value of one scaling factor based on physical reasoning, we obtain a minimization problem: There is only one free scaling factor in the conversion, and this factor can be assigned an optimal value that minimizes the condition number of the FE matrices.

##### 4.1. Scaling Factors

The transformation of the 12 EM quantities in the EM governing equations from the RCGS unit system to the GUS (or GEN) is as follows:

$$\text{GEN}_x = \beta_x \text{RCGS}_x, \quad \text{GEN}_t = \beta_t \text{RCGS}_t, \quad \text{GEN}_{mass} = \beta_m \text{RCGS}_{mass}, \quad \text{GEN}\mathbf{F} = \beta_F \text{RCGS}\mathbf{F}, \quad (4.1)$$

and

$$\begin{aligned} \text{GEN}\mathbf{D} &= \beta_D \text{RCGS}\mathbf{D}, & \text{GEN}\mathbf{E} &= \beta_E \text{RCGS}\mathbf{E}, & \text{GEN}\mathbf{P} &= \beta_P \text{RCGS}\mathbf{P}, \\ \text{GEN}\mathbf{H} &= \beta_H \text{RCGS}\mathbf{H}, & \text{GEN}\mathbf{B} &= \beta_B \text{RCGS}\mathbf{B}, & \text{GEN}\mathbf{M} &= \beta_M \text{RCGS}\mathbf{M}, \\ \text{GEN}\mathbf{J}_f &= \beta_J \text{RCGS}\mathbf{J}_f, & \text{GEN}\rho_f &= \beta_\rho \text{RCGS}\rho_f. \end{aligned} \quad (4.2)$$

The 12 multiplicative factors  $\beta_D, \dots, \beta_F$  are the dimensional scaling parameters to be determined using dimensional analysis. These scaling parameters are, however, not independent; they are related to each other via Maxwell's equations (which yield four relations), the constitutive laws (which yields four relations), the force equation (which yields two relations), and Newton's second law (which yields one relation). There is a total of  $4 + 4 + 2 + 1 = 11$  nonlinear relations for the 12 scaling parameters.

##### 4.2. Constrained Relations

If we compare the EM governing equations in the RCGS unit system in terms of dimensions to the equivalent equations in the GUS, the following relations that constrain the 12 scaling factors together are obtained:

- four relations derived from Maxwell's equations in dimensional form, i.e.,

$$\begin{aligned} [\text{curl } \mathbf{H}] &= \left[ \frac{1}{c} \mathbf{J}_f \right] \text{ gives the relation } \frac{\beta_J}{\beta_H} \beta_x = \frac{1}{c}, \\ [\text{curl } \mathbf{H}] &= \left[ \frac{1}{c} \frac{\partial \mathbf{D}}{\partial t} \right] \text{ gives the relation } \frac{\beta_D}{\beta_H} \frac{\beta_x}{\beta_t} = \frac{1}{c}, \\ [\text{curl } \mathbf{E}] &= \left[ \frac{1}{c} \frac{\partial \mathbf{B}}{\partial t} \right] \text{ gives the relation } \frac{\beta_B}{\beta_E} \frac{\beta_x}{\beta_t} = \frac{1}{c}, \\ [\text{div } \mathbf{D}] &= [\rho_f] \text{ gives the relation } \frac{\beta_\rho}{\beta_D} \beta_x = 1, \end{aligned} \quad (4.3)$$

where the square brackets  $[\cdot]$  indicate the dimension of the expression enclosed in these brackets;

- four relations from the constitutive laws (2.5), i.e.,

$$\frac{\beta_E}{\beta_D} = 1, \quad \frac{\beta_P}{\beta_D} = 1, \quad \frac{\beta_B}{\beta_H} = 1, \quad \frac{\beta_M}{\beta_H} = 1; \quad (4.4)$$

- two relations from the force equation (2.6)<sub>1</sub> and one relation from Newton's second law (2.6)<sub>2</sub>, i.e.,

$$\beta_\rho \beta_E = \frac{\beta_F}{\beta_x^3}, \quad \beta_J \beta_B = \frac{1}{c} \frac{\beta_F}{(\beta_x)^3}, \quad \beta_F = \frac{\beta_m \beta_x}{(\beta_t)^2}. \quad (4.5)$$

From Ampère's law (2.3), we have the dimensional relationships

$$[\text{RCGS curl}^{\text{RCGS}} \mathbf{H}] = \left[ \frac{1}{c} \text{RCGS} \mathbf{J}_f \right], \quad [\text{GEN curl}^{\text{GEN}} \mathbf{H}] = [\text{GEN} \mathbf{J}_f] \quad (4.6)$$

in the RCGS unit system and the GUS. From (4.1) and (4.2), the relationship for the quantities  $\mathbf{H}$ ,  $\mathbf{J}_f$ , and  $x$  between the RCGS unit system and the GUS are as follows:

$$\text{GEN} \mathbf{H} = \beta_H \text{RCGS} \mathbf{H}, \quad \text{GEN} \mathbf{J}_f = \beta_J \text{RCGS} \mathbf{J}_f, \quad \text{and} \quad \text{GEN} x = \beta_x \text{RCGS} x. \quad (4.7)$$

Dividing (4.6)<sub>1</sub> by (4.6)<sub>2</sub> and substituting (4.7) we obtain the relation  $\frac{\beta_J}{\beta_H} \beta_x = \frac{1}{c}$ , which is the result shown in (4.3)<sub>1</sub>. The derivation of the other 10 relations proceeds in a similar fashion.

### 4.3. Primary Scaling Parameters

With these 11 nonlinear constraint relations, we show that 10 of the 12 scaling parameters can be expressed in terms of the remaining two, called the two *primary* scaling parameters. The choice of the two primary scaling parameters should be made judiciously to reduce the complexity in the relations among the scaling parameters as much as possible. Further, the two primary scaling parameters should be independent of each other.

As an example of a *bad* choice of primary scaling parameters, consider the following two candidate primary scaling parameters:  $\beta_t$  and  $\beta_x$ . From (4.3)<sub>2</sub>, (4.3)<sub>3</sub>, (4.4)<sub>1</sub>, and (4.4)<sub>3</sub>, we obtain relation  $\beta_x/\beta_t = 1/c$ , which then shows that  $\beta_t$  and  $\beta_x$  are not independent, and thus invalidates their choice as primary scaling parameters.

From (4.4), we replace the scaling parameters  $\beta_D$  and  $\beta_P$  by  $\beta_E$ , and the scaling parameters  $\beta_H$  and  $\beta_M$  by  $\beta_B$  in (4.3), to obtain

$$\frac{\beta_J}{\beta_B} \beta_x = \frac{1}{c}, \quad \frac{\beta_E}{\beta_B} \frac{\beta_x}{\beta_t} = \frac{1}{c}, \quad \frac{\beta_B}{\beta_E} \frac{\beta_x}{\beta_t} = \frac{1}{c}, \quad \frac{\beta_\rho}{\beta_E} \beta_x = 1. \quad (4.8)$$

From (4.8)<sub>2</sub> and (4.8)<sub>3</sub>, we obtain

$$\beta_E = \pm \beta_B; \quad \frac{\beta_x}{\beta_t} = \pm \frac{1}{c}. \quad (4.9)$$

We have thus connected all the quantities in (4.4) via (4.9)<sub>1</sub>; i.e.,

$$\beta_E = \beta_D = \beta_P = \pm\beta_B = \pm\beta_H = \pm\beta_M. \quad (4.10)$$

Relation (4.10) essentially tells us that six of the scaling parameters  $\{\beta_E, \beta_D, \beta_P, \beta_B, \beta_H, \beta_M\}$  can be represented by a single scaling parameter among these six. Using (4.5)<sub>1</sub> in (4.8)<sub>4</sub> we obtain

$$\frac{\beta_x}{\beta_E} = \frac{\beta_E}{\beta_F/(\beta_x)^3} \Rightarrow \beta_E = \pm \frac{\sqrt{\beta_F}}{\beta_x}. \quad (4.11)$$

Relations (4.10) and (4.11) indicate that  $\beta_F$  and  $\beta_x$  are potentially good candidates as primary scaling parameters. Therefore, subsequently, we express all remaining scaling parameters—other than those in (4.10)—in terms of the two scaling parameters  $\beta_F$  and  $\beta_x$ . Using (4.5)<sub>2</sub> in (4.8)<sub>1</sub>, we obtain

$$\beta_J \beta_x = \frac{1}{c} \beta_B = \frac{1}{c} \frac{1}{c} \frac{1}{\beta_J} \frac{\beta_F}{(\beta_x)^3} \Rightarrow \beta_J = \pm \frac{1}{c} \frac{\sqrt{\beta_F}}{(\beta_x)^2}.$$

Substituting (4.11) in (4.8)<sub>4</sub>, we obtain

$$\beta_\rho = \frac{\beta_E}{\beta_x} = \pm \frac{\sqrt{\beta_F}}{(\beta_x)^2}.$$

From (4.5)<sub>3</sub>, we obtain

$$\beta_m = \frac{\beta_F (\beta_t)^2}{\beta_x} = c^2 \beta_F \beta_x.$$

The derived expressions can be summarized as follows:

$$\begin{aligned} \beta_E \equiv \beta_D \equiv \beta_P \equiv \beta_B \equiv \beta_H \equiv \beta_M &= \pm \frac{\sqrt{\beta_F}}{\beta_x}, \\ \beta_\rho &= \pm \frac{\sqrt{\beta_F}}{\beta_x^2}, \quad \beta_J = \pm \frac{1}{c} \frac{\sqrt{\beta_F}}{\beta_x^2}, \quad \beta_t = \pm c \beta_x, \quad \beta_m = c^2 \beta_F \beta_x. \end{aligned} \quad (4.12)$$

There are no more constraint relations other than the 11 used; thus  $\beta_F$  and  $\beta_x$  are indeed valid independent primary scaling parameters. The relations between the quantities in each of the unit systems are given in Table II.

*Remark 4.1.* Note that the numerical values that are assigned to the two scaling parameters  $\beta_F$  and  $\beta_x$  are relatively easier to give physical interpretation to than are most other scaling parameters. In fact, it will be shown that, by the structure of the finite element matrices, the condition number of these matrices is not affected by any (nonzero) value of  $\beta_F$ . Thus, we conveniently set  $\beta_F = 1$  to preserve the physical meaning of force during the unit conversion. Numerical values for  $\beta_x$  can be selected based on information on the geometric dimensions of the device.

The scaling parameters for the material properties  $\epsilon$ ,  $\mu$ , and  $\sigma$  are obtained from the relations

$$\mathbf{E} = \frac{1}{\epsilon} \mathbf{D}, \quad \mathbf{H} = \frac{1}{\mu} \mathbf{B}, \quad \mathbf{J}_f = \sigma \mathbf{E}. \quad (4.13)$$

**TABLE II**  
**Conversion of Symbols in Equations**

| Rationalized CGS    | Gaussian CGS                  | SI   | GUS (GEN)  |
|---------------------|-------------------------------|--|--|
| RCGS $q$            | CGS $q\sqrt{4\pi}$            | SI $q/\sqrt{\epsilon_0}$                     | $1/(\beta_x\sqrt{\beta_F})^{\text{GEN}} q$             |
| RCGS $\mathbf{D}$   | CGS $\mathbf{D}/\sqrt{4\pi}$  | $\sqrt{1/\epsilon_0}^{\text{SI}} \mathbf{D}$ | $\beta_x/\sqrt{\beta_F}^{\text{GEN}} \mathbf{D}$       |
| RCGS $\mathbf{E}$   | CGS $\mathbf{E}/\sqrt{4\pi}$  | $\sqrt{\epsilon_0}^{\text{SI}} \mathbf{E}$   | $\beta_x/\sqrt{\beta_F}^{\text{GEN}} \mathbf{E}$       |
| RCGS $\mathbf{J}_f$ | CGS $\mathbf{J}_f\sqrt{4\pi}$ | SI $\mathbf{J}_f/\sqrt{\epsilon_0}$          | $c \beta_x^2/\sqrt{\beta_F}^{\text{GEN}} \mathbf{J}_f$ |
| RCGS $\rho_f$       | CGS $\rho_f\sqrt{4\pi}$       | SI $\rho_f/\sqrt{\epsilon_0}$                | $\beta_x^2/\sqrt{\beta_F}^{\text{GEN}} \rho_f$         |
| RCGS $\mathbf{H}$   | CGS $\mathbf{H}/\sqrt{4\pi}$  | $\sqrt{\mu_0}^{\text{SI}} \mathbf{H}$        | $\beta_x/\sqrt{\beta_F}^{\text{GEN}} \mathbf{H}$       |
| RCGS $\mathbf{B}$   | CGS $\mathbf{B}/\sqrt{4\pi}$  | $\sqrt{1/\mu_0}^{\text{SI}} \mathbf{B}$      | $\beta_x/\sqrt{\beta_F}^{\text{GEN}} \mathbf{B}$       |
| RCGS $\mathbf{M}$   | CGS $\mathbf{M}\sqrt{4\pi}$   | $\sqrt{\mu_0}^{\text{SI}} \mathbf{M}$        | $\beta_x/\sqrt{\beta_F}^{\text{GEN}} \mathbf{M}$       |
| RCGS $\mathbf{P}$   | CGS $\mathbf{P}\sqrt{4\pi}$   | SI $\mathbf{P}/\sqrt{\epsilon_0}$            | $\beta_x/\sqrt{\beta_F}^{\text{GEN}} \mathbf{P}$       |
| RCGS $x$            | CGS $x$                       | SI $x$                                       | $^{\text{GEN}} x/\beta_x$                              |
| RCGS $t$            | CGS $t$                       | SI $t$                                       | $^{\text{GEN}} t/(c\beta_x)$                           |
| RCGS $mass$         | CGS $mass$                    | SI $mass$                                    | $^{\text{GEN}} mass/(c^2\beta_x\beta_F)$               |
| RCGS $F$            | CGS $F$                       | SI $F$                                       | $^{\text{GEN}} F/\beta_F$                              |
| RCGS $\epsilon$     | CGS $\epsilon$                | SI $\epsilon/\epsilon_0$                     | $^{\text{GEN}} \epsilon$                               |
| RCGS $\mu$          | CGS $\mu$                     | SI $\mu/\mu_0$                               | $^{\text{GEN}} \mu$                                    |
| RCGS $\sigma$       | $4\pi^{\text{CGS}} \sigma$    | SI $\sigma/\epsilon_0$                       | $c \beta_x^{\text{GEN}} \sigma$                        |
| RCGS $I$            | $\sqrt{4\pi}^{\text{CGS}} I$  | SI $I/\sqrt{\epsilon_0}$                     | $c/\sqrt{\beta_F}^{\text{GEN}} I$                      |
| RCGS $V$            | CGS $V/\sqrt{4\pi}$           | $\sqrt{\epsilon_0}^{\text{SI}} V$            | $1/\sqrt{\beta_F}^{\text{GEN}} V$                      |
| RCGS $C$            | $4\pi^{\text{CGS}} C$         | SI $C/\epsilon_0$                            | $^{\text{GEN}} C/\beta_x$                              |
| RCGS $L$            | CGS $L/(4\pi)$                | $\epsilon_0^{\text{SI}} L$                   | $^{\text{GEN}} L/(c^2\beta_x)$                         |
| RCGS $R$            | CGS $R/(4\pi)$                | $\epsilon_0^{\text{SI}} R$                   | $^{\text{GEN}} R/c$                                    |

The scaling parameters for the current  $I$  and for the voltage  $V$  are obtained from the relations

$$I = \int_{(\partial\Omega)_I} \mathbf{J}_f \cdot \hat{\mathbf{n}} d(\partial\Omega), \quad V = \int_{\mathcal{L}} \mathbf{E} \cdot \hat{\mathbf{t}} d\mathcal{L}. \quad (4.14)$$

The relations for the lumped parameters, i.e., the resistance  $R$ , the inductance  $L$ , and the capacitance  $C$ , are obtained from

$$R = V/I, \quad L = V \left/ \frac{dI}{dt} \right., \quad C = I \left/ \frac{dV}{dt} \right.. \quad (4.15)$$

Relations (4.13)–(4.15) remain unchanged in the RCGS unit system and in the GUS.

## 5. GENERALIZED UNIT SYSTEM (GUS)

We introduce the *generalized* unit system (GUS), and define the scaling parameters  $\alpha_x$  and  $\alpha_F$ , which can be used to transform the FE matrices to the GUS. The condition number of FE matrices in the GUS is related to the numerical values assigned to the scaling parameters  $\alpha_x$  and  $\alpha_F$ . We study the effects of transforming the FE matrices from the SI system to the GUS on static, transient, and time-harmonic problems. This transformation improves the condition number of the FE matrices for the transient and time-harmonic problems, and has no effect on the condition number of the FE matrices related to static problems.

### 5.1. Define a Unit System

To relate the numerical values of the quantities in the generalized unit system (GUS or GEN) to that in the other unit systems, we define the numerical (dimensionless) scaling parameter  $\alpha_x$  as follows:

$$\beta_x =: \alpha_x \frac{\text{generalized meter}}{\text{centimeter}}. \quad (5.1)$$

Recall from (4.1)<sub>1</sub> that  ${}^{\text{GEN}}x = \beta_x {}^{\text{RCGS}}x$ . To convert the length  ${}^{\text{RCGS}}x = 1$  centimeter to the length  ${}^{\text{GEN}}x$  in the GUS, we substitute  ${}^{\text{RCGS}}x = 1$  and use (5.1) to obtain

$${}^{\text{GEN}}x = \alpha_x \frac{\text{generalized meter}}{\text{centimeter}} 1 \text{ centimeter} = \alpha_x \text{ generalized meter}, \quad (5.2)$$

i.e.,

$$1 \text{ centimeter} \leftrightarrow \alpha_x \text{ generalized meter}. \quad (5.3)$$

We perform a similar process for the remaining 11 multiplicative factors  $\alpha_D, \dots, \alpha_F$ . We obtain the values for the remaining numerical multiplicative factors in terms of  $\alpha_F$  and  $\alpha_x$ , where

$$\beta_F =: \alpha_F \frac{\text{generalized dyne}}{\text{dyne}}.$$

Using  $\beta_F$  and  $\beta_x$  in (4.12), we obtain a conversion of the numerical values between the unit systems; the conversions between the most useful quantities are listed in Table III.

*Remark 5.1.* The multiplicative factor  $\alpha_F$  does not scale the matrices in the FE solution. This is because  $\alpha_F$  appears with equal powers in all terms involved in Maxwell's equations. The multiplicative factor  $\alpha_F$  simply cancels out in the ensuing FE formulation. Hence, a simplification used in the formulation for capacitors is to fix  $\beta_F := 1$  and obtain all the scaling parameters  $\beta$ 's in terms of  $\beta_x$ . Such a transformation preserves the physical meaning of force in the GUS to be the same as in other systems. The relations between the symbols in each of the unit systems is given in Table II with  $\beta_F = 1$ . The consequence of  $\beta_F := 1$  is  $\alpha_F = 1$ ; i.e., 1 dyne =: 1  ${}^{\text{GEN}}$ dyne. To obtain the numerical multiplicative factors  $\alpha$ 's for the other quantities in terms of  $\alpha_x$ , set  $\alpha_F = 1$  in Tables III.

### 5.2. Methods of Reducing the Condition Number of FE Matrices

The condition number of the finite element matrices are related to the following:

1. *Geometric dimensions* of the elements that constitute the FE model is critical to the condition number of the FE matrices. The main reason for *geometric* ill-conditioning is poor aspect ratio,<sup>6</sup> e.g., extremely thin electrodes interspersed with thick dielectric material.

2. A large change in *material properties*, in particular conductivity, contributes more toward ill-conditioning than geometric dimensions. For example, in passive EM devices, a mix between conductors and nonconductors leads to discontinuities in conductivity and induces ill-conditioning in the FE matrices.

<sup>6</sup> Aspect ratio is defined as the ratio between the largest edge and the smallest edge of an element. The thickness of the electrodes are on the order of 1.5  $\mu\text{m}$  and the thickness of the dielectric layers are on the order of 15.0  $\mu\text{m}$ .

**TABLE III**  
**Conversion of Numerical Values**

|                | Rationalized<br>CGS                          | Gaussian<br>CGS  | SI  | GUS  |
|----------------|--|--|---|--|
| $q$            | 1 statcoulomb                                | $\frac{1}{\sqrt{4\pi}}$ statcoulomb  | $\frac{10^{-9}}{3\sqrt{4\pi}}$ coulomb                                    | $\alpha_x \sqrt{\alpha_F}$ <sup>GEN</sup> coulomb  |
| $\mathbf{D}$   | $1 \frac{\text{statvolt}}{\text{cm}}$        | $\sqrt{4\pi} \frac{\text{statvolt}}{\text{cm}}$                                | $\frac{10^{-5}}{(3\sqrt{4\pi})}$ coulombs<br>m <sup>2</sup>               | $\frac{\sqrt{\alpha_F}}{\alpha_x}$ <sup>GEN</sup> volt<br>m  |
| $\mathbf{E}$   | $1 \frac{\text{statvolt}}{\text{cm}}$        | $\sqrt{4\pi} \frac{\text{statvolt}}{\text{cm}}$                                | $3 \times 10^4 \sqrt{4\pi} \frac{\text{volts}}{\text{m}}$                 | $\frac{\sqrt{\alpha_F}}{\alpha_x}$ <sup>GEN</sup> volt<br>m  |
| $\mathbf{J}_f$ | $1 \frac{\text{statampere}}{(\text{cm})^2}$  | $\frac{1}{\sqrt{4\pi}} \frac{\text{statampere}}{(\text{cm})^2}$                | $\frac{1}{3\sqrt{4\pi}} \times 10^{-5} \frac{\text{ampere}}{\text{m}^2}$  | $\frac{\sqrt{\alpha_F}}{3\alpha_x^2 \times 10^{10}}$ <sup>GEN</sup> ampere<br>( <sup>GEN</sup> m) <sup>2</sup> |
| $\rho_f$       | $1 \frac{\text{statcoulomb}}{(\text{cm})^3}$ | $\frac{\sqrt{\alpha_F}}{\sqrt{4\pi}} \frac{\text{statcoulomb}}{(\text{cm})^3}$ | $\frac{1}{3\sqrt{4\pi}} \times 10^{-3} \frac{\text{coulomb}}{\text{m}^3}$ | $\frac{\sqrt{\alpha_F}}{\alpha_x^2}$ <sup>GEN</sup> coulomb<br>( <sup>GEN</sup> m) <sup>3</sup>                |
| $\mathbf{H}$   | 1 oersted                                    | $\sqrt{4\pi}$ oersted  | $\frac{10^3}{\sqrt{4\pi}} \frac{\text{ampere-turns}}{\text{m}}$           | $\frac{\sqrt{\alpha_F}}{\alpha_x}$ <sup>GEN</sup> oersted  |
| $\mathbf{B}$   | 1 gauss                                      | $\sqrt{4\pi}$ gauss  | $\sqrt{4\pi} 10^{-4}$ tesla   | $\frac{\sqrt{\alpha_F}}{\alpha_x}$ <sup>GEN</sup> gauss  |
| $\mathbf{M}$   | 1 gauss                                      | $\frac{1}{\sqrt{4\pi}}$ gauss  | $\frac{10^3}{\sqrt{4\pi}}$ amperes<br>m                                   | $\frac{\sqrt{\alpha_F}}{\alpha_x}$ <sup>GEN</sup> gauss  |
| $\mathbf{P}$   | $1 \frac{\text{statcoulomb}}{(\text{cm})^2}$ | $\frac{1}{\sqrt{4\pi}} \frac{\text{statcoulomb}}{(\text{cm})^2}$               | $\frac{10^{-5}}{3\sqrt{4\pi}}$ coulomb<br>m <sup>2</sup>                  | $\frac{\sqrt{\alpha_F}}{\alpha_x}$ <sup>GEN</sup> coulomb<br>( <sup>GEN</sup> m) <sup>2</sup>                  |
| $x$            | 1 cm   | 1 cm   | $10^{-2}$ m   | $\alpha_x$ <sup>GEN</sup> m  |
| $t$            | 1 s  | 1 s  | 1 s   | $3\alpha_x \times 10^{10}$ <sup>GEN</sup> s  |
| $mass$         | 1 gm   | 1 gm   | $10^{-3}$ kg  | $9\alpha_x \alpha_F \times 10^{20}$ <sup>GEN</sup> gm  |
| $F$            | 1 dyne                                       | 1 dyne   | $10^{-5}$ newton  | $\alpha_F$ <sup>GEN</sup> dyne   |
| $\epsilon$     | 1 RCGS unit                                  | 1 CGS unit   | $\frac{1}{4\pi \times 9 \times 10^9}$ SI unit                             | 1 <sup>GEN</sup> units   |
| $\mu$          | 1 RCGS unit                                  | 1 CGS unit   | $4\pi \times 10^{-7}$ SI unit   | 1 <sup>GEN</sup> unit  |
| $\sigma$       | 1 RCGS unit                                  | $\frac{1}{4\pi}$ CGS unit  | $\frac{1}{4\pi \times 9 \times 10^9}$ SI unit                             | $\frac{1}{3\alpha_x \times 10^{10}}$ <sup>GEN</sup> unit   |
| $I$            | 1 statampere                                 | $\frac{1}{\sqrt{4\pi}}$ statampere   | $\frac{10^{-9}}{3\sqrt{4\pi}}$ ampere                                     | $\frac{\sqrt{\alpha_F}}{3 \times 10^{10}}$ <sup>GEN</sup> ampere   |
| $V$            | 1 statvolt                                   | $\sqrt{4\pi}$ statvolt   | $3\sqrt{4\pi} \times 10^2$ volt   | $\sqrt{\alpha_F}$ <sup>GEN</sup> volt  |
| $C$            | 1 statfarad                                  | $\frac{1}{4\pi}$ statfarad   | $\frac{10^{-11}}{9(4\pi)}$ farad  | $\alpha_x$ <sup>GEN</sup> farad  |
| $L$            | 1 stathenry                                  | $4\pi$ stathenry   | $9(4\pi) \times 10^{11}$ henry  | $9\alpha_x \times 10^{20}$ <sup>GEN</sup> henry  |
| $R$            | 1 statohm                                    | $4\pi$ statohm   | $9(4\pi) \times 10^{11}$ ohm  | $3 \times 10^{10}$ <sup>GEN</sup> ohm  |

In Section 3, the final matrix equations obtained via the FE formulation are linear equations of the form  $Ad = b$ , where  $A \in \mathbb{R}^{n \times n}$  is a nonsingular matrix,  $b \in \mathbb{R}^{n \times 1}$  is the right-hand side, and  $d \in \mathbb{R}^{n \times 1}$  is the solution. The condition number of the matrix  $A$  determines the numerical accuracy of the solution  $d$ . Here we present a method of “scaling” or “preconditioning” to alleviate the effects of poor condition numbers. Though we choose the method of *Gauss elimination* to demonstrate the effects of scaling, similar comments are applicable to other solution methods as well.

### 5.2.1. Preconditioning

One of the methods used to decrease the roundoff error is to “preprocess” matrix  $A$  before solution. This matrix preconditioning method scales the matrix  $A$  by pre- and

postmultiplying it by two selected matrices, thereby reducing its condition number [16]. Diagonal scaling, a standard preconditioning approach to improve the convergence of the iterative solver, has been widely used in various engineering applications [17–19]. Incomplete Cholesky factorization, first introduced in [18], has also been used as a preconditioning strategy. Unfortunately, only certain classes of positive definite matrices can be stably preconditioned by the incomplete Cholesky factorization [16].

Several new preconditioning methods were proposed recently to tackle the ill-conditioned linear systems [5, 20, 21]. In [5], to annihilate the effect of the extreme eigenvalues a deflated CG method is used. The convergence behavior of the CG method improves considerably and a reliable termination criterion is obtained. In [21] an effective preconditioner was proposed. However, an appropriate shift constant is difficult to find. The absence of a convenient and systematic procedure to construct the preconditioning matrices motivates changing of the traditional unit system to the generalized unit system. Unlike the previously mentioned preconditioning methods, if we start from preprocessing the resulting linear system matrices, our generalized unit system, inspired directly from the dimensional nature of physical problems, minimizes the condition number of the FE matrices and thus improves the numerical behavior of the solution procedure significantly.

### 5.2.2. Use of GUS

Motivated by the physics of the problem, we first describe the effects of scaling on the solution to a system of linear equations and then present a procedure to scale the FE matrix equations by changing the unit system used in Maxwell's equations, i.e., by changing  $\alpha_x$ . This approach can also be applied to a solution procedure using the Coulomb gauge.

*5.2.2.1. Static problems.* Recall from Table I that Gauss's law has an identical expression<sup>7</sup> in both the SI system and the GUS, i.e.,  ${}^{\text{SI}}\text{div} {}^{\text{SI}}\mathbf{D} - {}^{\text{SI}}\rho_f = 0$  and  ${}^{\text{GEN}}\text{div} {}^{\text{GEN}}\mathbf{D} - {}^{\text{GEN}}\rho_f = 0$ . Therefore, the FE matrix equations given in (3.5)

$$[{}^{\text{SI}}M^{\psi\psi}] \{ {}^{\text{SI}}\psi_0 \} = \{ {}^{\text{SI}}F^{\psi_0} \} \quad \text{and} \quad [{}^{\text{GEN}}M^{\psi\psi}] \{ {}^{\text{GEN}}\psi_0 \} = \{ {}^{\text{GEN}}F^{\psi_0} \} \quad (5.4)$$

look identical, with entries computed as

$${}^{\text{U}}M_{IJ}^{\psi\psi} := \int_{\text{U}\Omega, \Omega_{\text{cond}}} {}^{\text{U}}\epsilon ({}^{\text{U}}\text{grad } N_I) \cdot ({}^{\text{U}}\text{grad } N_J) d\Omega, \quad (5.5)$$

where  ${}^{\text{U}}$  represents both the SI system and the GUS. The numerical values for the entries of the FE matrices  $[{}^{\text{SI}}M^{\psi\psi}]$  and  $[{}^{\text{GEN}}M^{\psi\psi}]$  are, however, different. For a particular problem the numerical values of the entries in the matrix  $[{}^{\text{GEN}}M^{\psi\psi}]$  depend on the numerical scaling parameter  $\alpha_x$ . To derive a relation between the entries of the matrices in (5.5) for the SI and the generalized unit systems, we recall the following relations from Table III:

$$\begin{aligned} \text{for } x: 1 \text{ SI unit} &\equiv 10^2 \alpha_x \text{ GEN unit}, & \text{for } x^3: 1 \text{ SI unit} &\equiv 10^6 (\alpha_x)^3 \text{ GEN unit}, \\ \text{for grad: } 1 \text{ SI unit} &\equiv \frac{1}{10^2 (\alpha_x)} \text{ GEN unit}, & \text{for } \epsilon: 1 \text{ SI unit} &\equiv \frac{1}{\epsilon_0} \text{ GEN unit}. \end{aligned} \quad (5.6)$$

<sup>7</sup> Without a left superscript, the unit system used is implicitly the SI system.

Hence,

$$\begin{aligned}
& \int_{\text{SI}\Omega \setminus \Omega_{\text{cond}}} \text{SI}\epsilon (\text{SI}\text{grad} N_I) \cdot (\text{SI}\text{grad} N_J) d\Omega \\
& \equiv \frac{1}{\epsilon_0} \frac{1}{10^2 \alpha_x} \frac{1}{10^2 \alpha_x} (10^2 \alpha_x)^3 \int_{\text{GEN}\Omega \setminus \Omega_{\text{cond}}} \text{GEN}\epsilon (\text{GEN}\text{grad} N_I) \cdot (\text{GEN}\text{grad} N_J) d\Omega \\
& \equiv \frac{10^2 \alpha_x}{\epsilon_0} \int_{\text{GEN}\Omega \setminus \Omega_{\text{cond}}} \text{GEN}\epsilon (\text{GEN}\text{grad} N_I) \cdot (\text{GEN}\text{grad} N_J) d\Omega; \tag{5.7}
\end{aligned}$$

i.e.,

$$[\text{SI}M^{\psi\psi}] = \frac{(\alpha_x \times 10^2)}{\epsilon_0} [\text{GEN}M^{\psi\psi}]. \tag{5.8}$$

Upon transforming the matrix from the SI system to the GUS, all entries of the matrix  $[\text{SI}M^{\psi\psi}]$  are multiplied equally by the scaling factor  $\epsilon_0/(\alpha_x \times 10^2)$ . Hence, the ratio of the largest to the smallest eigenvalue, i.e., the condition number, remains the same in both unit systems.

Recall from Table I that Ampère's law has an identical expression in both the SI system and the GUS; i.e.,  $\text{SI}\text{curl}\text{SI}\mathbf{H} - \text{SI}\mathbf{J}_a = 0$  and  $\text{GEN}\text{curl}\text{GEN}\mathbf{H} - \text{GEN}\mathbf{J}_a = 0$ . Therefore the corresponding FE matrix equations given in (3.6)

$$[\text{SI}K^{AA}]\{\text{SI}\mathcal{A}_0\} = \{\text{SI}F^{A_0}\} \quad \text{and} \quad [\text{GEN}K^{AA}]\{\text{GEN}\mathcal{A}_0\} = \{\text{GEN}F^{A_0}\} \tag{5.9}$$

look identical, with entries computed as

$${}^U K_{IJ}^{AA} := \int_{U\Omega} \frac{1}{U\mu} ({}^U\text{grad} N_I \cdot {}^U\text{grad} N_J) \mathbf{1} d\Omega - \int_{U\Omega} \frac{1}{U\mu} ({}^U\text{grad} N_J \otimes {}^U\text{grad} N_I) d\Omega, \tag{5.10}$$

where  ${}^U$  represents both the SI system and the GUS. For a particular problem, the numerical values of the entries in the matrix  $[\text{GEN}K^{AA}]$  depend on the numerical scaling parameter  $\alpha_x$ . We recall the following relations from Table III:

$$\text{for curl: } 1 \text{ SI unit} \equiv \frac{1}{10^2(\alpha_x)} \text{GEN unit}, \quad \text{for } \mu: 1 \text{ SI unit} \equiv \frac{1}{\mu_0} \text{GEN unit}.$$

Hence,

$$\begin{aligned}
& \int_{\text{SI}\Omega} \frac{1}{\text{SI}\mu} (\text{SI}\text{grad} N_I) \cdot (\text{SI}\text{grad} N_J) d\Omega \\
& \equiv \mu_0 \frac{1}{10^2 \alpha_x} \frac{1}{10^2 \alpha_x} (10^2 \alpha_x)^3 \int_{\text{GEN}\Omega} \frac{1}{\text{GEN}\mu} (\text{GEN}\text{grad} N_I) \cdot (\text{GEN}\text{grad} N_J) d\Omega \\
& \equiv \mu_0 10^2 \alpha_x \int_{\text{GEN}\Omega} \frac{1}{\text{GEN}\mu} (\text{GEN}\text{grad} N_I) \cdot (\text{GEN}\text{grad} N_J) d\Omega \tag{5.11}
\end{aligned}$$

and

$$\begin{aligned}
& \int_{\text{SI}\Omega} \frac{1}{\text{SI}\mu} (\text{SI}\text{grad} N_J) \otimes (\text{SI}\text{grad} N_I) d\Omega \\
& \equiv \mu_0 10^2 \alpha_x \int_{\text{GEN}\Omega} \frac{1}{\text{GEN}\mu} (\text{GEN}\text{grad} N_J) \otimes (\text{GEN}\text{grad} N_I) d\Omega; \tag{5.12}
\end{aligned}$$



i.e.,

$$[{}^{\text{SI}}K^{AA}] = \mu_0 \alpha_x \times 10^2 [{}^{\text{GEN}}K^{AA}]. \quad (5.13)$$

Similar to electrostatic problems, upon transforming the matrix from the SI system to the GUS, all entries of the matrix  $[{}^{\text{GEN}}K^{AA}]$  are multiplied throughout by the scaling factor  $1/(\mu_0 10^2 \alpha_x)$ . Hence, the condition number remains the same in both unit systems.

*5.2.2.2. Transient problems.* Using Table III we obtain relations between the FE matrices given in Section 3 in the SI unit system and in the GUS for the transient problems. For example, consider the matrix  $M^{AA}$  defined in (3.16). Using (5.6) we obtain

$$\int_{{}^{\text{SI}}\Omega} {}^{\text{SI}}\epsilon_{N_I} \cdot N_J \, d\Omega \equiv \frac{(10^2 \alpha_x)^3}{\epsilon_0} \int_{{}^{\text{GEN}}\Omega} {}^{\text{GEN}}\epsilon_{N_I} \cdot N_J \, d\Omega; \quad (5.14)$$

i.e.,  ${}^{\text{SI}}M^{AA} = [(\alpha_x \times 10^2)^3 / \epsilon_0] {}^{\text{GEN}}M^{AA}$ . Similarly, we obtain the following relations for the other matrices in (3.17). The mass matrix  $M$  and the damping matrix  $B$ , represented by  $Y$  as

$$\begin{bmatrix} {}^{\text{SI}}Y^{AA} & {}^{\text{SI}}Y^{A\psi} \\ {}^{\text{SI}}Y^{\psi A} & {}^{\text{SI}}Y^{\psi\psi} \end{bmatrix} = \frac{1}{a\epsilon_0} \begin{bmatrix} (\alpha_x \times 10^2)^3 {}^{\text{GEN}}Y^{AA} & (\alpha_x \times 10^2)^2 {}^{\text{GEN}}Y^{A\psi} \\ (\alpha_x \times 10^2)^2 {}^{\text{GEN}}Y^{\psi A} & (\alpha_x \times 10^2) {}^{\text{GEN}}Y^{\psi\psi} \end{bmatrix}, \quad (5.15)$$

where  $a = 1$  for the  $M$  matrix and  $a = c\alpha_x$  for the  $B$  matrix, and the stiffness matrix

$$\begin{bmatrix} {}^{\text{SI}}K^{AA} & 0 \\ 0 & 0 \end{bmatrix} = \mu_0 \begin{bmatrix} (\alpha_x \times 10^2) {}^{\text{GEN}}K^{AA} & 0 \\ 0 & 0 \end{bmatrix} \quad (5.16)$$

are related by the length scaling parameters numerical multiplicative factor  $\alpha_x$ . Different values of  $\alpha_x$  result in different generalized unit systems. Using these relations, we can relate the matrix (3.14) in the GUS to that in the SI system as

$$\begin{aligned} [{}^{\text{GEN}}\mathbb{K}] &:= \left( \frac{1}{({}^{\text{GEN}}\Delta t_{n+1})^2 \beta} \begin{bmatrix} {}^{\text{GEN}}M^{AA} & {}^{\text{GEN}}M^{A\psi} \\ {}^{\text{GEN}}M^{\psi A} & {}^{\text{GEN}}M^{\psi\psi} \end{bmatrix} \right. \\ &\quad \left. + \frac{\gamma}{{}^{\text{GEN}}\Delta t_{n+1} \beta} \begin{bmatrix} {}^{\text{GEN}}B^{AA} & {}^{\text{GEN}}B^{A\psi} \\ {}^{\text{GEN}}B^{\psi A} & {}^{\text{GEN}}B^{\psi\psi} \end{bmatrix} + \begin{bmatrix} {}^{\text{GEN}}K^{AA} & 0 \\ 0 & 0 \end{bmatrix} \right) \\ &= \frac{\epsilon(c\alpha_x)^2}{({}^{\text{SI}}\Delta t_{n+1})^2 \beta} \begin{bmatrix} \frac{1}{(\alpha_x \times 10^2)^3} {}^{\text{SI}}M^{AA} & \frac{1}{(\alpha_x \times 10^2)^2} {}^{\text{SI}}M^{A\psi} \\ \frac{1}{(\alpha_x \times 10^2)^2} {}^{\text{SI}}M^{\psi A} & \frac{1}{(\alpha_x \times 10^2)} {}^{\text{SI}}M^{\psi\psi} \end{bmatrix} \\ &\quad + \frac{(c\epsilon)(c\alpha_x)\gamma}{{}^{\text{SI}}\Delta t_{n+1} \beta} \begin{bmatrix} \frac{\alpha_x}{(\alpha_x \times 10^2)^3} {}^{\text{SI}}B^{AA} & \frac{\alpha_x}{(\alpha_x \times 10^2)^2} {}^{\text{SI}}B^{A\psi} \\ \frac{\alpha_x}{(\alpha_x \times 10^2)^2} {}^{\text{SI}}B^{\psi A} & \frac{\alpha_x}{(\alpha_x \times 10^2)} {}^{\text{SI}}B^{\psi\psi} \end{bmatrix} \\ &\quad + \frac{1}{\mu_0} \begin{bmatrix} \frac{1}{\alpha_x \times 10^2} {}^{\text{SI}}K^{AA} & 0 \\ 0 & 0 \end{bmatrix}. \end{aligned} \quad (5.17)$$

For the problem at hand, the material properties and the geometry of the domain  $\Omega$  are fixed, and hence the FE matrices in the SI unit system are fixed for a given discretization. However, changing the value for  $\alpha_x$  can improve the condition number of the matrix  $\mathbb{K}$  in

the GUS. In theory, we could find an optimal value for  $\alpha_x$  to minimize the condition number of the dynamic stiffness matrix  ${}^{\text{GEN}}\mathbb{K}$  in the GUS, i.e.,

$$\alpha_x^{\text{opt}} := \min_{\alpha_x \neq 0} (\text{condition number of } {}^{\text{GEN}}\mathbb{K}), \quad (5.18)$$

where  $\alpha_x^{\text{opt}}$  is the optimal scaling parameter. Numerically, we could construct a coarse mesh for the problem at hand, and vary  $\alpha_x$  to find an approximate optimal value.

*5.2.2.3. Time-harmonic problems.* The relationships (5.15) to (5.16) for the mass, damping, and stiffness matrices are the same for the time-harmonic problem. This similarity implies that the condition number of the matrix

$$[\overline{{}^{\text{GEN}}\mathbb{K}}] := \begin{bmatrix} {}^{\text{GEN}}rK - ({}^{\text{GEN}}\omega^2) {}^{\text{GEN}}rM & ({}^{\text{GEN}}\omega) {}^{\text{GEN}}iB \\ -({}^{\text{GEN}}\omega) {}^{\text{GEN}}rB & {}^{\text{GEN}}iK - ({}^{\text{GEN}}\omega^2) {}^{\text{GEN}}iM \end{bmatrix} \quad (5.19)$$

can be changed by varying the numerical scaling factor  $\alpha_x$ . Note that for the frequency we have the conversion  ${}^{\text{SI}}\omega = (1/c\alpha_x) {}^{\text{GEN}}\omega$ . Similarly to transient problems, we can find an optimal value for  $\alpha_x$  to minimize the condition number of the matrix  $\overline{{}^{\text{GEN}}\mathbb{K}}$ , i.e.,

$$\alpha_x^{\text{opt}} := \min_{\alpha_x \neq 0} (\text{condition number of } \overline{{}^{\text{GEN}}\mathbb{K}}), \quad (5.20)$$

where  $\alpha_x^{\text{opt}}$  is the optimal scaling parameter.

The effects of scaling depend on the excitation frequency. At very low frequencies, Maxwell's equations require a solution only to an uncoupled problem. For an uncoupled problem, where the vector potential  $\mathbf{A}$  and the scalar potential  $\psi$  are solved separately, scaling has no effect. Hence, scaling is most effective for problems at higher frequencies.

## 6. NUMERICAL EXAMPLES

We apply the proposed multiple-scale technique to a simple parallel plate capacitor shown in Fig. 1a. The dimensions of the parallel plate capacitor are equal to the single cell in an MLCC [7, 9]. The parallel plate capacitor considered here does not have the positive and negative vias of the single cell; the top and bottom electrodes are flat rectangular plates. The electrodes have a footprint of  $0.635 \times 0.635$  cm, and are  $1.5\text{-}\mu\text{m}$  thick. The dielectric in between is  $15\text{-}\mu\text{m}$  thick. The conducting material used for the electrodes and the vias is silver palladium, and the dielectric material is a ceramic such as barium titanate. The material properties for the electrode and the dielectric are listed in Table IV.

**TABLE IV**  
**Material Properties for the MLCC in the SI Unit System**

| Material          | Permittivity $\epsilon$<br>(farad/m) | Permeability $\mu$<br>(henry/m) | Conductivity $\sigma$<br>(1/(ohm-m)) |
|-------------------|--------------------------------------|---------------------------------|--------------------------------------|
| Dielectric        | $1500\epsilon_0$                     | $\mu_0$                         | 0.0                                  |
| Electrodes & Vias | $\epsilon_0$                         | $1.0008\mu_0$                   | $2.9412 \times 10^6$                 |
| Bus               | $\epsilon_0$                         | $0.999991\mu_0$                 | $5.8 \times 10^7$                    |
| Air               | $\epsilon_0$                         | $1.000004\mu_0$                 | 0.0                                  |

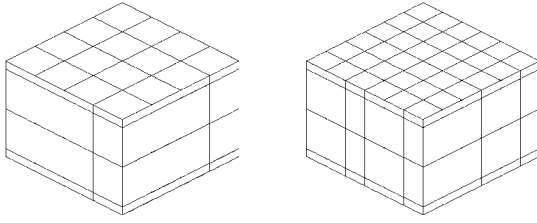


**FIG. 2.** Meshes for the parallel plate capacitor: The mesh is refined along the horizontal plane. See Table V for details.

A voltage is applied at the top plane of the top electrode and the bottom plane of the bottom electrode. The electric and magnetic fields are determined by solving the coupled electromagnetic problem; i.e., the matrix equation (3.11) is solved for each time step in the transient solution. Similarly, the matrix equation is solved for each frequency to determine the time-harmonic solution.

As explained in Section 4, using the multiple-scale technique reduces the condition number of the FE matrices, thereby increasing the accuracy of the solution. We examine the effect on the condition number with changing mesh size. The capacitor shown in Fig. 2 is discretized using four different meshes. The number of nodes for the four meshes shown in Fig. 2 range from 20 nodes for mesh (a) to 245 nodes for mesh (d). Table V lists the number of nodes, the number of elements, and the unconstrained degrees of freedom in the FE solution. Figure 3 shows the effect of changing the mesh size and varying the scaling factor  $\alpha_x$  for the transient and the time-harmonic solutions, respectively. We observe that the mesh size does not significantly affect the choice of the optimal scaling factor  $\alpha_x^{\text{opt}}$ . We conclude for this particular example that  $\alpha_x^{\text{opt}} \approx 10^3$  for the transient and time-harmonic solutions. Hence, in practice, we could choose the optimal scaling factor  $\alpha_x^{\text{opt}}$  from a coarse mesh and use it for a refined mesh. We also observe that the condition number increases with an increase in the number of degrees of freedom in the solution. The condition number shows a significant improvement from the SI system of units to the generalized system of units for both the transient and the time-harmonic solutions; see Table VI for details. The relative error improves significantly for the time-harmonic solution: For mesh (d) we observe in Table VI that the relative error improves from  $\mathcal{O}(10^{-5})\%$  in the SI unit system to  $\mathcal{O}(10^{-11})\%$  in the optimal GUS. In the transient problem, where the related matrices are

**TABLE V**  
**The Specifications of the Different Meshes Used to Solve the Parallel Plate Capacitor Problem**

| Mesh | Number of nodes | Number of elements | Degrees of freedom |               |
|------|-----------------|--------------------|--------------------|---------------|
|      |                 |                    | Transient          | Time-harmonic |
| (a)  | 20              | 4                  | 64                 | 128           |
| (b)  | 45              | 16                 | 144                | 288           |
| (c)  | 125             | 64                 | 400                | 800           |
| (d)  | 245             | 144                | 784                | 1568          |

*Note.* The different meshes are shown in Fig. 2.

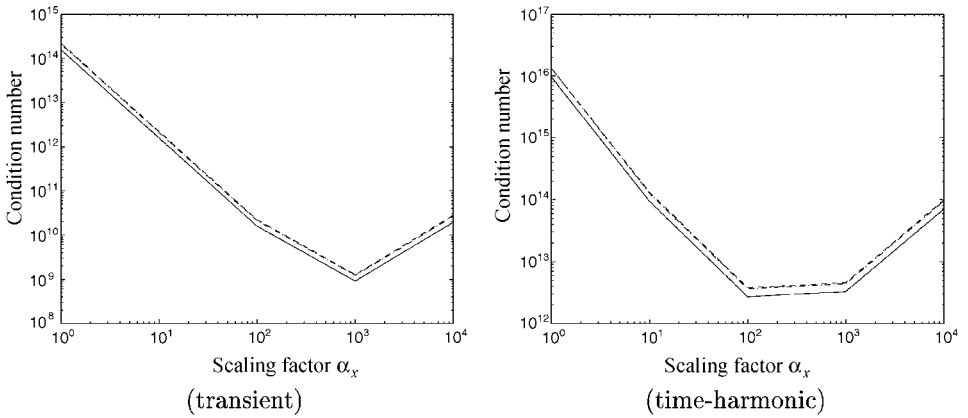


**FIG. 3.** The change in the condition number with changing mesh size and varying scaling factor  $\alpha_x$ . The solid line, the dashed line, the dashed-dotted line, and the dotted line are for meshes (a), (b), (c), and (d) in Table V, respectively.

symmetric, the relative error (see Footnote 4) was already minimal before rescaling and thus did not decrease further after rescaling, even though there was a significant decrease in the condition number as a result of rescaling. On the other hand, in the time-harmonic problem, where the related matrices are nonsymmetric, the relative error was much larger (by an order of  $10^{12}$ ) before rescaling, and thus it decreased significantly (together with the condition number) after rescaling.

In Fig. 4 we examine the effects of change in the time step size for transient solutions and change in frequency for the time-harmonic solutions. It is evident that the optimal scaling factor  $\alpha_x^{\text{opt}}$  depends on the time step size and on the frequency. For transient solutions (Fig. 4a), at smaller time step size, numerical differences among the coefficients

**TABLE VI**  
**The Condition Number and Relative Error for the Parallel Plate Capacitor Problem**

| Mesh                    | SI unit system        |                        | Generalized unit system<br>( $\alpha_x = 10^3$ ) |                        |
|-------------------------|-----------------------|------------------------|--|------------------------|
|                         | Condition number      | Relative error         | Condition number                                 | Relative error         |
| Transient solutions     |                       |                        |  |                        |
| (a)                     | $8.75 \times 10^{18}$ | $2.40 \times 10^{-17}$ | $9.10 \times 10^8$                               | $1.05 \times 10^{-17}$ |
| (b)                     | $1.15 \times 10^{19}$ | $1.95 \times 10^{-17}$ | $1.22 \times 10^9$                               | $1.95 \times 10^{-17}$ |
| (c)                     | $1.70 \times 10^{19}$ | $1.43 \times 10^{-17}$ | $1.27 \times 10^9$                               | $1.02 \times 10^{-17}$ |
| (d)                     | $1.80 \times 10^{19}$ | $1.53 \times 10^{-17}$ | $1.34 \times 10^9$                               | $1.41 \times 10^{-17}$ |
| Time-harmonic solutions |                       |                        |  |                        |
| (a)                     | $5.21 \times 10^{20}$ | $2.17 \times 10^{-5}$  | $3.27 \times 10^{12}$                            | $1.05 \times 10^{-11}$ |
| (b)                     | $2.74 \times 10^{21}$ | $6.26 \times 10^{-5}$  | $4.39 \times 10^{12}$                            | $9.48 \times 10^{-11}$ |
| (c)                     | $2.40 \times 10^{20}$ | $7.08 \times 10^{-5}$  | $4.58 \times 10^{12}$                            | $1.96 \times 10^{-10}$ |
| (d)                     | $2.55 \times 10^{20}$ | $8.04 \times 10^{-5}$  | $4.52 \times 10^{12}$                            | $2.06 \times 10^{-10}$ |

*Note.* The different meshes are shown in Fig. 2.

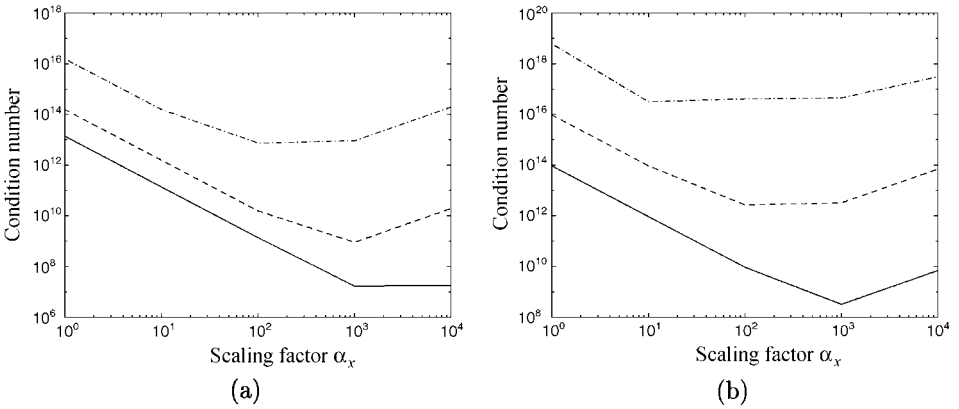


**FIG. 4.** The change in the condition number with varying scaling factor  $\alpha_x$ . In (a), the transient solution, the solid line, the dashed line, and the dashed-dotted line are with the time step size  $\Delta t_{n+1} = 2\pi/10^9$  SI units,  $\Delta t_{n+1} = 2\pi/10^7$  SI units, and  $\Delta t_{n+1} = 2\pi/10^5$  SI units, and in (b), the time-harmonic solution, the solid dashed, and dashed-dotted lines are with angular frequency  $\omega = 10^9$  SI units,  $\omega = 10^7$  SI units, and  $\omega = 10^5$  SI units, respectively.

$(1/\mu)$ ,  $\sigma/\Delta t_{n+1}$ , and  $\epsilon/\Delta t_{n+1}^2$  of the FE matrices (5.17) are smaller, and we obtain smaller condition numbers. Similarly, for time-harmonic solutions (Fig. 4b), at higher frequencies, the numerical differences among the coefficients  $(1/\mu)$ ,  $\sigma\omega$ , and  $\epsilon\omega^2$  of the FE matrices (5.19) are smaller, and we obtain smaller condition numbers. Moreover, the optimal scaling factor  $\alpha_x^{\text{opt}}$  changes with frequency. For example, in a time-harmonic solution,  $\alpha_x^{\text{opt}} \approx 10^1$  for  $\omega = 10^5$ , and  $\alpha_x^{\text{opt}} \approx 10^3$  for  $\omega = 10^9$ .

The properties of the material, i.e., the conductivity  $\sigma$ , permittivity  $\epsilon$ , and the permeability  $\mu$ , affects the choice of an optimal scaling factor. Figure 5 (condition number) and Fig. 6 (relative error) show the effects of changing the conductivity with the SI unit system and the GUS. It is evident that a higher conductivity and lower frequency degrade the condition of the solution in the SI unit system and the use of the multiple-scaling technique is imperative to avoid numerical ill-conditioning.

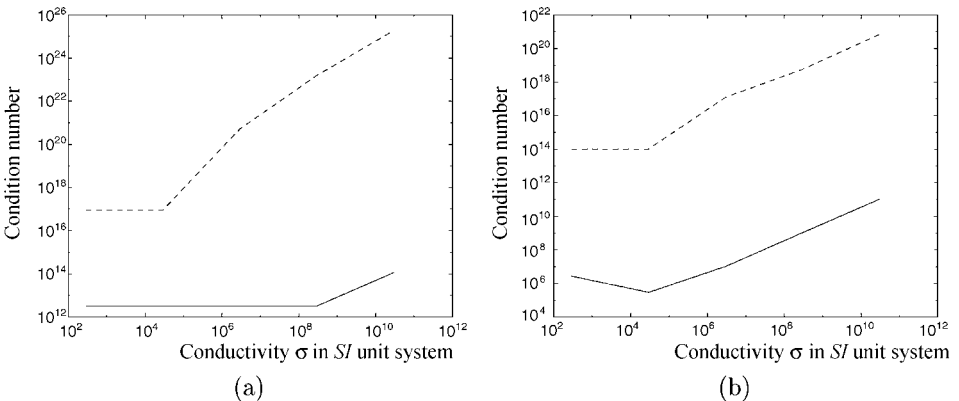


**FIG. 5.** The change in the condition number with varying conductivity  $\sigma$  of the electrode at angular frequency (a)  $\omega = 10^7$  SI units and (b)  $\omega = 10^{11}$  SI units. The solid line is with the GUS ( $\alpha_x = 10^3$ ), and the dashed line is with the SI unit system.

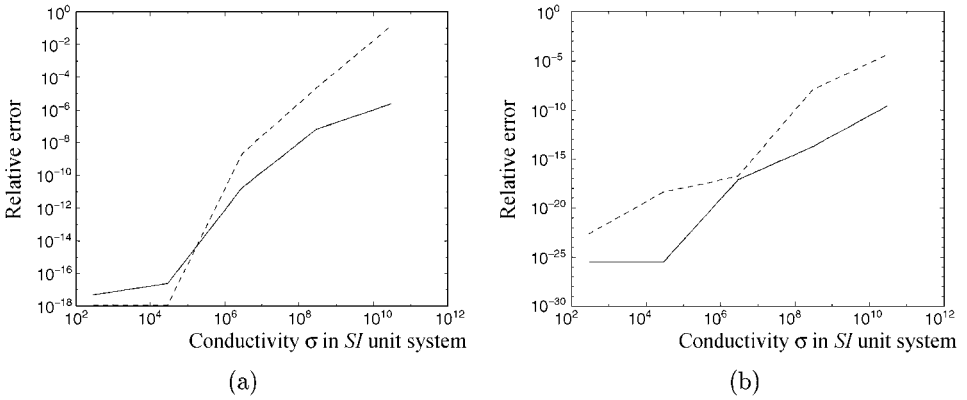


**FIG. 6.** The change in the *relative error* with varying conductivity  $\sigma$  of the electrode at angular frequency (a)  $\omega = 10^7$  SI units and (b)  $\omega = 10^{11}$  SI units. The solid line is with the GUS ( $\alpha_x = 10^3$ ), and the dashed line is with the SI unit system.

## 7. CLOSURE

We have introduced a new multiple-scale technique to model electromagnetic systems. Our new multiple-scale technique, which leads to our proposed generalized unit system, offers the flexibility of choosing an effective interaction between the different physical processes. We nondimensionalize and scale Maxwell's equations to a new *generalized* system of units. Numerical factors that are related to the physical properties of vacuum in Maxwell's equations and in the constitutive laws are eliminated since they are absorbed into the field quantities in the scaling process. This decreases the condition number of the matrices in the FE solution, and we thereby reduce the error significantly.

The scaling parameter is decided by the geometry and material properties of the electromagnetic device components. The multiple-scale technique permits a change in the scaling parameter and, hence, is easily adapted to components with a variety of geometrical shapes and material properties.

Numerical examples showed that the multiple-scale technique can significantly reduce the condition number of the FE matrices, thereby increasing the accuracy of the solution. We also conclude that scaling improves the condition number of the FE matrix in both transient and time-harmonic problems. However, only solutions to time-harmonic problems show a significant improvement in accuracy. We also studied the effects of mesh refinement on the choice of an optimal scaling factor  $\alpha_x^{\text{opt}}$ . We conclude that  $\alpha_x^{\text{opt}}$  is not significantly affected by mesh refinement. However, the scaling factor  $\alpha_x^{\text{opt}}$  depends on the excitation frequency and the material properties.

The application of the proposed GUS is not restricted to the stiff problem encountered in the case of the example studied here.

## ACKNOWLEDGMENT

The authors are thankful for the research support of the National Science Foundation.

## REFERENCES

1. A. Nicolet, F. Delince, N. Bamps, A. Genon, and W. Legros, A coupling between electric circuits and 2d magnetic field modeling, *IEEE Trans. Magn.* **29**(2), 1697 (1993).

2. R. K. Wangsness, *Electromagnetic Fields*, 2nd ed. (Wiley, New York, 1986).
3. V. Rojansky, *Electromagnetic Fields and Waves* (Dover, New York, 1979).
4. W. Morweiser, G. Meunier, and H. Salze, Computer-aided design of passive multilayer components using electromagnetic field computation, *IEEE Trans. Components, Packag. Manuf. Technol. A* **17**(3), 338 (1994).
5. C. Vuik, A. Segal, and J. A. Meijerink, An efficient preconditioned CG method for the solution of a class of layered problems with extreme contrasts in the coefficients, *J. Comput. Phys.* **152**, 385 (1999).
6. B. E. MacNeal, Ed., *MSC/EMAS Modeling Guide* (The MacNeal–Schwendler Corp., Los Angeles, 1989).
7. K. D. T. Ngo, Lumped parameter model for a multilayer ceramic capacitor, Private Communication (1992).
8. K. D. T. Ngo, Multilayer capacitor suitable for substrate integration and multimegahertz filtering, US Patent No. 4,949,217.
9. L. Vu-Quoc, V. Srinivas, and Y. Zhai, Finite element analysis of advanced multilayer capacitors: Field computation and postprocessing for lumped parameters, *Int. J. Numer. Methods Eng.*, to appear, 2002.
10. P. P. Silvester and R. L. Ferrari, *Finite Elements for Electrical Engineers* (Cambridge Univ. Press, New York, 1983).
11. J. Jin, *The Finite Element Method in Electromagnetics* (Wiley, New York, 1993).
12. G. A. Maugin, The method of virtual power in continuum mechanics: Applications to coupled fields, *Acta Mech.* **35**, 1 (1980).
13. T. J. R. Hughes, *The Finite Element Method* (Prentice–Hall, Englewood Cliffs, NJ, 1987).
14. O. C. Zienkiewicz and R. L. Taylor, *The Finite Element Method*, 4th ed. (McGraw–Hill, New York, 1989).
15. B. E. MacNeal, J. R. Brauer, and R. N. Coppelino, A general finite element vector potential formulation of electromagnetics using a time-integrated electric scalar potential, *IEEE Trans. Magn.* **26**(5), 1768 (1990).
16. G. H. Golub and C. F. van Loan, *Matrix Computations* (Johns Hopkins Univ. Press, Baltimore, 1987).
17. R. K. Coomer and I. G. Graham, Massively parallel methods for semiconductor device modelling, *Computing* **56**(1), 1 (1996).
18. R. E. Alcouffe, A. Brandt, J. E. Dendy, Jr., and J. W. Painter, The multigrid method for diffusion equations with strongly discontinuous coefficients, *SIAM J. Sci. Stat. Comput.* **2**(4), 430 (1981).
19. M. J. Hagger, *Iterative Solution of Large, Sparse Systems of Equations, Arising in Groundwater Flow Models*, Ph.D. thesis (University of Bath, 1995).
20. F. X. Canning and J. F. Scholl, Diagonal preconditioners for the EFIE using a wavelet basis, *IEEE Trans. Antenna Propagation* **44**(9), 1239 (1996).
21. H. J. Kim, K. Choi, and H. B. Lee, A new algorithm for solving ill-conditioned linear systems, *IEEE Trans. Magn.* **32**(3), 1373 (1996).